

## Assessment of the radio $^3\text{H-CH}_4$ tracer technique to measure aerobic methane oxidation in the water column

Ingeborg Bussmann,<sup>\*1</sup> Anna Matousu,<sup>2,3</sup> Roman Osudar,<sup>1</sup> Susan Mau<sup>4</sup>

<sup>1</sup>Alfred Wegener Institute, Helmholtz Centre for Polar and Marine Research, 27498 Helgoland, Germany

<sup>2</sup>Faculty of Sciences, University of South Bohemia, Branišovská 1760, 370 05 České Budějovice, Czech Republic

<sup>3</sup>Biology Centre of the Czech Academy of Sciences, Institute of Hydrobiology, Na Sádkách 7, 370 05 České Budějovice, Czech Republic

<sup>4</sup>MARUM Center for Marine Environmental Sciences and Department of Geosciences, University of Bremen, 28359 Bremen, Germany

### Abstract

Microbial methane oxidation rates in ocean and freshwater systems reveal how much of emitted methane from the sediments is oxidized to  $\text{CO}_2$  and how much can reach the atmosphere directly. The tracer-method using  $^3\text{H-CH}_4$  provides a way to measure methane oxidation rates even in water with low methane concentrations. We assessed this method by implementing several experiments, collecting data from various environments, and including recent literature concerning the method to identify any uncertainties that should be considered. Our assessment reveals some difficulties of the method but also reassures previous assumptions to be correct. Some of the difficulties are hardly to be avoided, such as incubating all samples at the right in situ temperature or limiting the variability of methane oxidation rate measurements in water of low methanotrophic activity. Other details, for example, quickly measuring the total radioactivity after stopping the incubation, are easy to adapt in each laboratory. And yet other details as shaking during incubation and bottle size seem to be irrelevant. With our study, we hope to improve and to encourage future measurements of methane oxidation rates in different environments and to provide a standard procedure of methane oxidation rate measurements to make the data better comparable.

### Introduction

Measurements of methane oxidation (MOX) rates are essential to understand why the large input of methane into oceans, lakes, rivers is in opposition to the relatively low flux of the gas to the atmosphere (Reeburgh 2007). Methane ( $\text{CH}_4$ ) is after water vapor and  $\text{CO}_2$ , the most important greenhouse gas with a global warming potential that exceeds carbon dioxide ( $\text{CO}_2$ ) 34-fold over a 100 yr timescale (IPCC, 2013). Methane is produced in aquatic sediments as well as in the water itself. In sediments, methane is generated by microbial breakdown as the last step of anaerobic degradation of organic matter (biogenic methane) and by thermocatalytic processes by increased temperature and pressure in deeply buried sediments [thermogenic methane (Tissot and Welte 1984)]. In the water column of the ocean, methane production has been linked to methylphosphonic acid (Karl et al. 2008; Metcalf et al. 2012) and dimethylsulfoniopropio-

nate (Damm et al. 2010) as substrates for methanogenesis, as well as to anaerobic microenvironments (Reeburgh 2007). Also in the water column of lakes an until now unknown process of methane production in oxygenated water has been suggested based on incubation experiments and isotope analysis (Tang et al. 2014).

Despite of all these methane sources only little of the gas actually escapes to the atmosphere. About 11 Tg  $\text{CH}_4 \text{ yr}^{-1}$  is emitted to the atmosphere from the ocean (Bange et al. 1994) contributing 2% to the  $\sim 550 \text{ Tg CH}_4 \text{ yr}^{-1}$  from all natural and anthropogenic sources (IPCC, 2013). A similar quantity of  $40 \text{ Tg yr}^{-1}$  (range 8–73  $\text{Tg yr}^{-1}$ ) originates from freshwater sources like rivers, lakes, and reservoirs (Bastviken et al. 2011; IPCC, 2013). These limited quantities are thought to be due to microbial oxidation of the gas in the water, which maintains the bulk of the ocean at low nanomolar concentrations (Reeburgh 2007).

Aerobic MOX is realized by methanotrophs, who oxidize methane with oxygen to  $\text{CO}_2$  and water. Methane oxidizing bacteria are found in oxic sediments and in the water column of most marine and freshwater settings, where oxygen is available (Jensen et al. 1992; Ding and Valentine 2008;

Additional Supporting Information may be found in the online version of this article.

\*Correspondence: Ingeborg.bussmann@awi.de

**Table 1.** Comparison of the main characteristics of  $^3\text{H}$  labeled methane vs.  $^{14}\text{C}$ -labeled methane.

	$^3\text{H}$ -methane	$^{14}\text{C}$ -methane
Reaction	$^3\text{H-CH}_4 + 2\text{O}_2 \Rightarrow \text{CO}_2 + 2\ ^3\text{H-H}_2\text{O}$	$^{14}\text{C-CH}_4 + 2\text{O}_2 \Rightarrow ^{14}\text{C-CO}_2 + 2\text{H}_2\text{O} + ^{14}\text{C - biomass}$
Specific activity	High ( $0.37\text{--}0.74\ \text{TBq mmol}^{-1}$ ), thus, $< 3\ \text{nmol L}^{-1}$ methane are added to a water sample	Low ( $37\text{--}185\ \text{MBq mmol}^{-1}$ ), thus, $< 500\ \text{nmol L}^{-1}$ methane are added to a water sample
Tracer storage	Limited tracer storage due to decomposition of the tracer over time	No problems with tracer storage known to date
Lab-equipment	GC for methane concentrations Liquid scintillation counter for radioactivities.	GC for methane concentrations Liquid scintillation counter for radioactivities. Tube furnace and shaker for quantification of $^{14}\text{C-CH}_4$ and $^{14}\text{C-CO}_2$ Filtering devices for biomass determination.
Environment	Applicable to aerobic environments only	Applicable to aerobic and anaerobic environments
Exemption limit	Higher exemption limit	Lower exemption limit
Ionization energy	Low ionization energy (19 keV), thus, possible interference with chemo luminescence	Higher ionization energy (156 keV) less interference with chemo luminescence

Rahalkar et al. 2009; Tsutsumi et al. 2012). Aerobic methanotrophic bacteria have been classified as type I and type II methanotrophs based on their phylogenetic position, carbon assimilation pathways, and the arrangement of intracellular membranes, and they belong to the classes *Gammaproteobacteria* and *Alphaproteobacteria*, respectively (Bowman 2006). Reported turnover times of methane range from 100s of years in the open ocean (Jones 1991; Angelis et al. 1993) to several years in the coastal seas (Heintz et al. 2012) and to days in freshwater environments (Abril and Iversen 2002). Besides the aerobic oxidation of methane, it can also be oxidized in the absence of oxygen, that is, in sediments and in anoxic waters. Especially the oxidation in sediments by mostly archaea but also some bacteria plays an important role in reducing the methane flux from the sediment into the water column (Krüger et al. 2005).

Several techniques have been implemented to qualify and quantify the microbial methane consumption. MOX can be measured by the decrease of methane concentration over time (Scranton and Brewer 1978; Abril et al. 2007), the change in isotopic composition (Bastviken et al. 2002) or by a combination of stable isotope and conservative tracer measurements (Rehder et al. 1999; Heeschen et al. 2004). However, adding a radioactive tracer such as  $^3\text{H-CH}_4$  (Valentine et al. 2001; Mau et al. 2013) or  $^{14}\text{C-CH}_4$  (Reeburgh et al. 1992; Pack et al. 2011) makes quantification more sensitive.

Especially the method using  $^3\text{H-CH}_4$  has become more and more established over the last decade as sample processing requires only a few steps, which can be carried out on board a research vessel, the tracer has become commercially available, and it has several advantages compared to  $^{14}\text{C-CH}_4$  (Table 1).  $^3\text{H-CH}_4$  has a higher specific activity ( $3.7\text{--}7.4 \times$

$10^{11}\ \text{Bq mmol}^{-1}$ ) than  $^{14}\text{C-CH}_4$  with  $3.7\text{--}18 \times 10^7\ \text{Bq mmol}^{-1}$ . Thus, the methane concentration of a water sample is changed by  $< 3\ \text{nmol l}^{-1}\ ^3\text{H-CH}_4$  whereas the addition of  $^{14}\text{C-CH}_4$  increases methane concentration of a sample by up to  $500\ \text{nmol l}^{-1}$ . This significantly alters the concentration of the gas especially in samples collected from environments with low in situ methane concentrations. However, recently also a low-level  $^{14}\text{C-CH}_4$  method has been proposed, where  $^{14}\text{C}$  is measured with accelerator mass spectrometry (Pack et al. 2011). Furthermore, the  $^3\text{H-CH}_4$  has the advantage of a higher permitted radioactivity ( $10^9\ \text{Bq}$ ) compared to  $^{14}\text{C}$  with  $10^7\ \text{Bq}$ , which can be transported without special license (German Radiation Protection Ordinance, 2001, and ADR 2.2.7.1.1, Tab. 2.2.7.2.2.1, U.S. DoT, CFR Part 173.436). The working limits seem to differ in each country, thus, we will not give further information here. For transportation with ships, documents according to the IMO are recommended (IMO class 7, UN number 2910). For transportation with airplanes, documents according to the IATA are recommended (IATA DGR 10.3.1, Tab 10.3.A).

Regardless of the radiotracer, more and more often tracer incubations are conducted on board of research vessels, where similar to any laboratory country specific radiation regulations apply. The transport of the radioactive tracer, radioactive samples, and radioactive waste has to be organized according to these safety regulations. Ideally, the handling is done in an isotope van, especially if other parties of a cruise are interested in the natural abundance of  $^3\text{H}$  or  $^{14}\text{C}$ . Areas on deck, where incubations are carried out, should be monitored for potential spills on a regular basis and these areas should be regularly hosed. This is particularly important on small vessels with too little space for an isotope van.

Furthermore, sufficient ventilation should be assured by an open window, open door, or working outside if no ventilation hood is provided. Of principle importance are regular wipe tests to screen for any potential contaminations. With sufficient care the radiotracer technique provides a great tool to investigate and quantify microbial methane oxidation.

Although we describe here a rather established method, we felt the need to publish an extensive testing of the method to get the best results for current and future users. The idea arose during the Pergamon workshop in Kiel in 2011 where several parties met to discuss MOX rate measurements. Every user tested the method by implementing different experiments. Here, we summarize the tests to make the method of measuring MOX by adding  $^3\text{H-CH}_4$  more comparable between laboratories, to facilitate it for newcomers and also to report on the little tricks and pitfalls hidden in the detail of every method.

### Material and methods

To test parts of the MOX rate measurements using  $^3\text{H-CH}_4$  as tracer, we followed the general method described below. Deviations and verifications of this protocol are indicated in the assessment part.

#### Methane oxidation rate

Water is sampled directly from Niskin bottles attached to a CTD/rosette. A 10–20 cm long tubing, which fits to the stop-cock of the Niskin bottle and reaches to the bottom of the sampling bottle, is used to collect water from the water-sampling device. Water samples are collected in 12–160 mL glass bottles by filling the bottle from the bottom to the top and flushing the bottle twice to minimize contact of the sampled water with the surrounding air, that is, avoiding changes of the in situ methane and oxygen concentrations. The glass bottles are then closed avoiding air bubbles with rubber stoppers and are crimp sealed. Several water samples have to be collected: two to three bottles for determination of MOX rates, one bottle as killed control, and one to two bottles for analysis of in situ methane concentrations.

After crimp sealing of the water sample, the radioactive tracer is added to the sample and poisoned control bottles.  $^3\text{H-CH}_4$  (as gas), commercially available from Biotrend (Köln, Germany) or from American Labeled Chemicals (St. Louis) is added by syringe using a second needle to allow for displacement of water. The amount of added  $^3\text{H-CH}_4$ -tracer has to be adapted to the environment, it should be high enough to produce a measurable quantity of  $^3\text{H-H}_2\text{O}$ , and as low as possible, to minimize any significant methane concentration changes in the water sample.

The addition of the  $^3\text{H-CH}_4$  is  $>1000$  Bq resulting in methane addition in the pico molar range ( $10^{-12}$  mol). After injection of the  $^3\text{H-CH}_4$ , all bottles are vigorously shaken for at least 30 s to equilibrate the gaseous tracer with the liquid phase.

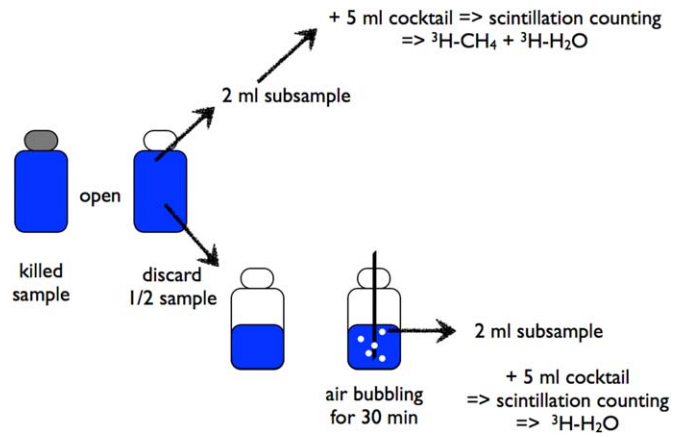


**Fig. 1.** Scheme for analysis of the  $^3\text{H}$ -radioactivity in the total fraction and in the water fraction of a sample (or control bottle).

The samples are then incubated in the dark at near in situ temperature. After incubation for hours until days, microbial activity is stopped by poisoning or the samples are directly processed.

Then the total radioactivity ( $^3\text{H-CH}_4$  and  $^3\text{H-H}_2\text{O}$ ) added to the sample and the product of the oxidation,  $^3\text{H-H}_2\text{O}$ , have to be measured in the sample and control bottles (Fig. 1). To determine the total radioactivity of the sample, the sample bottle (or control bottle) is opened and 1–2 mL subsample is pipetted into a seven milliliter scintillation vial. Five milliliter scintillation cocktail is added to the subsample. The scintillation cocktail should be specific for  $^3\text{H}$ -samples and aqueous solutions (e.g., Ultima Gold LLT from Perkin Elmer). Scintillation cocktail and sample are mixed by shaking the scintillation vial and counted in a liquid scintillation counter. This can be a laboratory-based counter (e.g., from Perkin Elmer) or a small, transportable one (e.g., Triathler from Hidex, Finland). Decays per minute (dpm) are calculated by the instruments based on the efficiency determined from the internal quench correction and calibration.

After counting the total radioactivity ( $^3\text{H-CH}_4$  and  $^3\text{H-H}_2\text{O}$ ) of the sample, the  $^3\text{H-CH}_4$  is removed from the sample and the remaining  $^3\text{H-H}_2\text{O}$  counted. For the removal of the  $^3\text{H-CH}_4$ , part of the sample is discarded to prevent overflow when sparging the sample with nitrogen or air. A synthetic air or a nitrogen gas bottle is connected to a sparging device that consists of several long needles or tubes to process more than one sample at a time. During expeditions, we also used an aquarium pump. The needles or tubes should reach nearly to the bottom of the bottle (i.e., be  $\sim 10$ -mm long) and the tubes should have a small diameter ( $\sim 1$  mm) to leave sufficient space for ventilation at the neck of the bottle. After sparging the sample for at least 30 min, a 1–2 mL subsample is mixed with five milliliter scintillation cocktail in a seven milliliter scintillation vial and counted in a liquid scintillation counter.

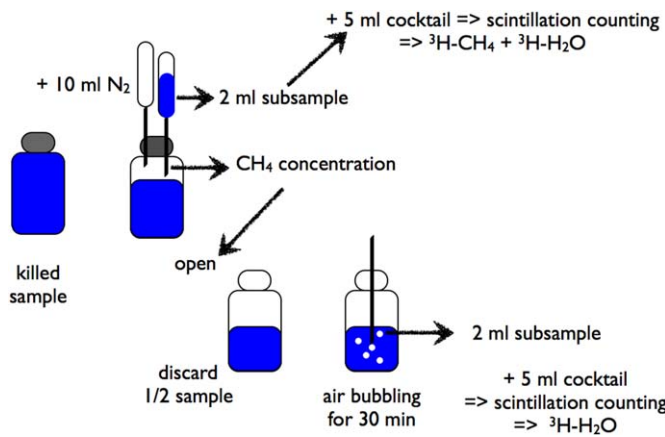


**Fig. 2.** Modified scheme for measuring the methane concentration in the sample bottle, before assessing the radioactive fractions.

### Methane concentration

To calculate the MOX rate, the methane concentration of the respective sample has to be known. Commonly, an additional water sample is collected from the same Niskin bottle and poisoned to stop microbial MOX. The sample is then stored cold until methane concentration analysis.

However, if the samples were manipulated by adding different amounts of  $^3\text{H-CH}_4$  or plain  $\text{CH}_4$ , it is necessary to measure the methane concentration in each sample before measuring its radioactivity (Fig. 2). Therefore, a 10 mL syringe without piston is inserted into the killed sample (120–160 mL sample). With a second syringe 10 mL of nitrogen are injected into the sample bottle while water flows into the syringe without piston assuring atmospheric pressure conditions in the sample bottle. Part of this water is used for measurement of the total radioactivity ( $^3\text{H-CH}_4$  and  $^3\text{H-H}_2\text{O}$ ; see above). The sample bottle with headspace is shaken and left standing for at least one day to equilibrate. An aliquot of the headspace is then analyzed with a gas chromatograph (GC) equipped with a flame ionization detector to determine the methane concentration.

### Calculation

After measuring methane concentration, the total radioactivity ( $^3\text{H-CH}_4$  and  $^3\text{H-H}_2\text{O}$ ) and the radioactivity of the produced water ( $^3\text{H-H}_2\text{O}$ ), turnover time ( $\tau$  in d) and MOX rates ( $\text{nmol l}^{-1} \text{d}^{-1}$ ) can be calculated assuming first-order kinetics (Valentine et al. 2001):

$$k' = ({}^3\text{H-H}_2\text{O}/({}^3\text{H-CH}_4 + {}^3\text{H-H}_2\text{O}))/t \quad (1)$$

$$\text{MOX} = k' \times [\text{CH}_4]_{\text{in situ}} \quad (2)$$

$$\tau = 1/k' = [\text{CH}_4]/\text{MOX} \quad (3)$$

where  $k'$  is the first-order rate constant calculated as the fraction of  $^3\text{H-CH}_4$  oxidized per unit time ( $t$ ) and  $[\text{CH}_4]_{\text{in situ}}$  is the ambient methane concentration in  $\text{nmol L}^{-1}$ . The methane concentration should be measured in separate bottles,

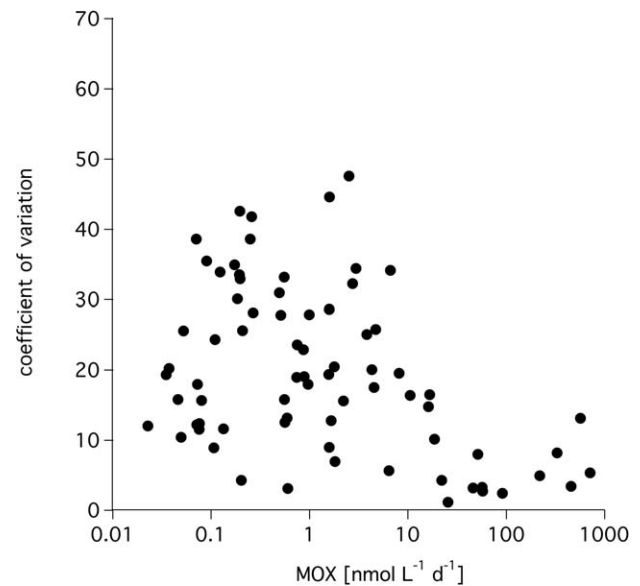


**Fig. 3.** Coefficients of variation of triplicate samples in relation to MOX rates collected during eight research cruises in the North Sea and in the Elbe in 2013.

without tracer addition.  $k'$  was termed the pseudo first-order rate constant for the methane transport into the cells at constant cell population by Button (1991). The turnover time can also be seen as an indication of the relative activity of various water samples as described by Koschel (1980).

The radioactivity of the  $^3\text{H-H}_2\text{O}$  fraction in the killed controls is used to check for the amount of not biologically produced water. In case this background value is  $>1\%$  the radioactivity of the total fraction, it should be subtracted from the sample value (Jørgensen 1978). In marine waters about 0.1% of the injected tracer was found to be “abiotic water.” In freshwaters the percentage can increase to about 5%.

### Statistics

Wilcoxon Rank Sign Tests for nonparametric data were performed with Kaleidagraph 4.1.

### Assessment

#### Number of replicates

Replicates are essential to obtain a good estimate of MOX rates. Commonly, 2–3 replicates are used to quantify MOX rates (Schubert et al. 2010; Mau et al. 2013). To test the quality of data obtained from triplicate measurements, the coefficient of variation ( $\text{cv} = \text{standard deviation} \times 100/\text{mean}$ ) was calculated for data collected during eight cruises in the North Sea and Elbe in 2013. Our results show that the coefficient of variations is rather high ( $23\% \pm 11\%$ ,  $n = 58$ ) at low activities ( $< 10 \text{ nmol l}^{-1} \text{d}^{-1}$ ) and lower ( $7\% \pm 5\%$ ,  $n = 17$ ) at higher activities ( $> 10 \text{ nmol l}^{-1} \text{d}^{-1}$ ; Fig. 3). For comparison, when measuring the bacterial production in the water



column using the leucine incorporation method, the coefficient of variation ranges from 6% to 10%, with 3–4 replicates (Ducklow et al. 2012; Simon et al. 2012). Hence, if a better precision and discriminatory power is needed, for example, when comparing different experimental setups, more than three replicates are necessary. The precision of replicates describes the total error of MOX rates. This total error consists of the error of each step of the method and the heterogeneity of the methanotrophic population in the water sample. All the tested error causes evaluated below, thus, most likely affect low rate measurements more than high rate measurements.

### Bottle size

Glass bottles of different sizes (25–160 mL) are used to measure aerobic MOX rates. While larger samples contain a higher absolute number of bacteria, and thus, might be more representative, small sample vials have laboratory advantages. Less tracer has to be added to smaller samples, less space is needed during incubation, and less radioactive waste is produced. To test if small sample volumes are representative or if the coefficient of variation increases due to the small sample volume, a batch of North Sea water was filled in 12–160 mL glass bottles and incubated as described above. The comparison of incubation of different sample volumes showed no significant differences in turnover times (Wilcoxon Rank Sum Test,  $n=5$ ). Therefore, small water samples are adequate, at least in waters with a turnover time of less than 20 d.

### Stoppers

There are several different rubber stoppers available to firmly close the sample bottles. The stoppers should be gas tight to prevent any losses of methane and at the same time should be “soft” enough to allow easy handling with needles. However, most of the commercially available rubber stoppers leach organic and inorganic contaminants, which can inhibit or limit MOX. An extensive study was conducted by Niemann et al. (2015) recommending halogenated butyl rubber stoppers.

### Adding the $^3\text{H-CH}_4$ tracer

The tracer can be added to the sample as a small bubble of concentrated  $^3\text{H-CH}_4$  (10  $\mu\text{L}$ ) or as a bigger bubble (100  $\mu\text{L}$ ) diluted with nitrogen. According to the ratio of surface to volume of a sphere, more gas is diluted from small bubbles than from large ones. Furthermore, large bubbles may result in stripping of methane from the sample into the bubble in case of methane rich waters. However, handling of a 10  $\mu\text{L}$  volume in contrast to a 100  $\mu\text{L}$  volume is rather tricky especially on a moving boat. Furthermore, using diluted tracer has the advantage that the rate of decomposition is decreased. To test the effect of the bubble size, North Sea water was incubated with a 10  $\mu\text{L}$  and a 100  $\mu\text{L}$  bubble containing  $131 \pm 40$  Bq and  $190 \pm 23$  Bq, respectively ( $n=10$  each, 24 h, at ambient methane concentration of 15 nmol

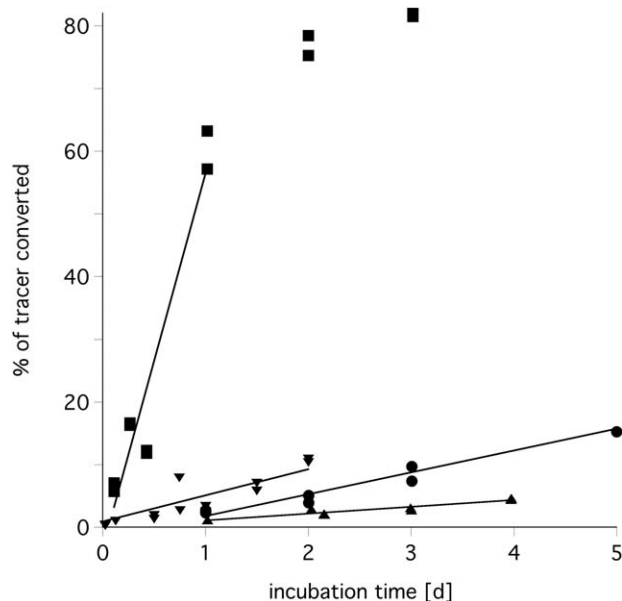


**Fig. 4.** Time series conducted by incubating samples from different environments for 0.1–5 d. Freshwater from the pond of the MPI-Bremen (squares) and seawater from Storfjorden, Svalbard (circles), the North Sea (upward triangle), and the Santa Barbara Basin (downward triangle).

$\text{l}^{-1}$  at  $18^\circ\text{C}$ ). The turnover time of the 10  $\mu\text{L}$  samples ( $5.1 \pm 0.4$  d) was slightly higher than the turnover time of the 100  $\mu\text{L}$  samples ( $4.5 \pm 0.4$  d). The difference is in the range of the error of replicates indicating that the enhanced solubility for the 10  $\mu\text{L}$  sample was negligible.

### Incubation time

The incubation time has to be adapted to each environment. The time period should be long enough to produce a measurable amount of  $^3\text{H-H}_2\text{O}$  and as short as possible to minimize incubation artefacts such as decomposition of the  $^3\text{H-CH}_4$  or isotopic exchange reactions. To test the appropriate incubation time, one or more time series should be conducted. A time series is implemented by taking water samples from one location and incubating duplicate or triplicate samples for 3 h, 6 h, 12 h, 1 d, 2 d, etc. However, during field campaigns such time series may be difficult to perform due to the lack of time, space, or counting instruments. To provide a general idea of appropriate incubation times, we compiled data of time series of freshwater and marine environments. Our compilation suggests incubation times of  $<24$  h in freshwater and 1–3 d in marine systems (Fig. 4). The time series indicate that  $^3\text{H-CH}_4$  uptake per time is linearly related as long as the substrate (methane) is not limited. In case of the freshwater sample, the linear relation (first-order kinetics) is given during the first day of incubation and in case of the seawater samples over up to 5 d.

### During the incubation

Incubation conditions for rate measurements should mimic the natural environment to determine a rate that

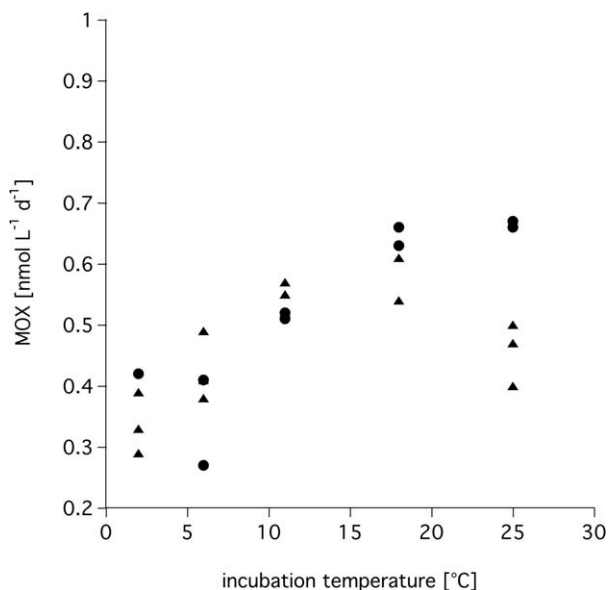


**Fig. 5.** Influence of the incubation temperature on the MOX rate. North Sea water (triangles) and Elbe water (circles) with in situ methane concentrations of  $20 \text{ nmol L}^{-1}$  and  $32 \text{ nmol L}^{-1}$ , respectively, were incubated for 24 h at different temperatures. Water samples were collected in January 2011 and had in situ temperatures of  $3^\circ\text{C}$ .

resembles as close as possible the in situ rate. Typically, water samples are incubated at near in situ temperature, in the dark, and without motion.

In a set of experiments, we assessed the influence of temperature on the MOX rate. Elbe and North Sea water samples that were incubated at temperatures from  $2^\circ\text{C}$  to  $25^\circ\text{C}$  show the temperature curve of the MOX reaction (Fig. 5). We determined the  $Q_{10}$ -factor, which indicates the temperature dependence of a process: according to Raven and Geider (1988):

$$Q_{10} = \exp(-10 \times m \div T_{is}^2)$$

where  $T_{is}$  is the in situ temperature and  $m$  the slope of the regression line of the Arrhenius plot (the inverse of the absolute temperature vs. the natural logarithm of the MOX rate). We calculated  $Q_{10}$  values to range between 1.52 and 1.75, for Elbe and North Sea water, respectively. These values are in accordance with  $Q_{10}$  values between 1.4 and 2.1 determined for MOX rates in northern peatlands by (Dunfield et al. 1993). Also,  $Q_{10}$  values of 1–1.84 were reported for ammonia oxidation in a marine setting (Horak et al. 2013).  $Q_{10} > 1$  indicates that the reaction rate increases with increasing temperature. Therefore, incubation temperature should be as close as possible to the in situ temperature or should be corrected if one wants to determine the in situ MOX rate.

Samples are generally incubated in the dark; even though the influence of light on microbial MOX is unknown. Some studies suggest an inhibitory effect of light on methanotrophic growth and activity (Dumestre et al. 1999). Other studies suggest that the inhibitory effect depends on type of

methanotrophs (Osudar et al. unpublished data). Unless more knowledge is available, we recommend to incubate the samples in the dark and also to minimize samples processing under high laboratory light.

The influence of motion/shaking of a sample during the incubation was tested. The motion not only increases the solubility of the tracer bubble but also imitates the motion of a research vessel at sea. The 120 mL sample bottles were put on a rocker during incubation to move the tracer bubble along the side of the bottle. No significant difference was found between samples from the rocker and samples incubated without motion ( $n = 5$  each). Also, the coefficient of variation was not different. Shaking of the sample is, thus, not necessary during incubation.

### Stopping the incubation

If immediate analysis of samples after incubation is impracticable, a “killing” substance to stop microbial activity has to be added to the sample. This can be a toxic substance or a substance that shifts the pH. Strong toxic substances are mercury chloride ( $\text{HgCl}_2$ ) and sodium azide ( $\text{NaN}_3$ ), which both require environmental safe disposal. Sulfuric acid ( $\text{H}_2\text{SO}_4$ ) or sodium hydroxide solution ( $\text{NaOH}$ ) can be used to shift the pH and to stop microbial activity. We compiled data of the different “killing” substances in Table 2, which shows the amount of  $^3\text{H-H}_2\text{O}$  in the killed control as percent of the total radioactivity ( $^3\text{H-CH}_4$  and  $^3\text{H-H}_2\text{O}$ ). In seawater samples, we observed 2–15 times as high counts in control samples using  $\text{NaN}_3$  in contrast to  $\text{HgCl}_2$  (Table 2). For  $\text{HgCl}_2$ , it should be noted that some methanotrophs may be able to reduce  $\text{HgCl}_2$  to elemental Hg, but they need to use most of the energy that they gain from methane metabolism to fuel mercury (II) reduction (Boden et al. 2011). Therefore, especially methanotrophs might not be stopped by adding  $\text{HgCl}_2$ . In seawater both  $\text{NaOH}$  and  $\text{H}_2\text{SO}_4$  can be used to poison the samples. The  $^3\text{H-H}_2\text{O}$  radioactivity of the controls using  $10 \text{ mol L}^{-1}$   $\text{NaOH}$  was  $1.0\% \pm 0.3\%$  ( $n = 35$ ) in North Sea water, while 25%  $\text{H}_2\text{SO}_4$  had a slightly better performance (Table 2). In freshwater in most cases  $5 \text{ mol L}^{-1}$   $\text{NaOH}$  was superior to 25%  $\text{H}_2\text{SO}_4$  in stopping the samples (Experiments I and II in Table 2). Field data revealed a low residual activity when stopping with  $5 \text{ mol L}^{-1}$   $\text{NaOH}$  (Elbe river near Hamburg; Lake Constance). However, in some cases (Czech part of the Elbe)  $\text{NaOH}$  was not sufficient and best results were obtained with concentrated  $\text{H}_2\text{SO}_4$  (96%; Table 2). Overall  $\text{H}_2\text{SO}_4$  was the best killing reagent, with a better performance than  $\text{NaOH}$ , which in turn is advantageous compared to  $\text{HgCl}_2$  and  $\text{NaN}_3$  that are both environmentally hazardous. In the marine environment diluted (25%)  $\text{H}_2\text{SO}_4$  was sufficient, whereas in freshwater concentrated  $\text{H}_2\text{SO}_4$  appears to be superior.

After stopping the incubation, the samples should be analyzed as soon as possible. Experiments with storage time of  $^3\text{H-CH}_4$ -labeled samples show that within the first week there is a significant loss of  $^3\text{H-CH}_4$ , while the  $^3\text{H-H}_2\text{O}$

**Table 2.** Field and experimental data on the influence of the stopping reagent on the amount of  $^3\text{H-H}_2\text{O}$  in the killed control as percent of the total radioactivity ( $^3\text{H-CH}_4$  and  $^3\text{H-H}_2\text{O}$ ). Given are the averages  $\pm$  standard deviation and the number of samples in brackets. The experiments were performed with water from the Elbe near Hamburg and North Sea water near Helgoland. We added 0.2–0.3 mL of base or acid to 120 mL sample bottles, resulting in a pH of  $< 1.5$  or  $> 10$ .

Location/ experiment		5M NaOH	10 mol L <sup>-1</sup> NaOH	25% H <sub>2</sub> SO <sub>4</sub>	95% H <sub>2</sub> SO <sub>4</sub>	HgCl <sub>2</sub>	NaN <sub>3</sub>
Seawater	Santa Barbara					0.1 $\pm$ 0.0 (6)	0.5 $\pm$ 0.2 (6)
Seawater	North Sea		1.0 $\pm$ 0.3 (35)	0.1 $\pm$ 0.2 (39)			
Freshwater	Elbe near Hamburg	3.8 $\pm$ 4.0 (37)					
Freshwater	Elbe near Prague	8.5 $\pm$ 2.6 (12)		9.5 $\pm$ 4.5 (12)	0.8 $\pm$ 1.7 (31)		
Freshwater	Lake Constance	5.2 $\pm$ 7.1 (50)					
Freshwater	Exp. I	5.4 $\pm$ 1.0 (4)		37.9 $\pm$ 0.3 (4)			
Seawater		0.2 $\pm$ 0.1 (4)		0.0 $\pm$ 0.0 (4)			
Freshwater	Exp. II	0.4 $\pm$ 0.1 (3)		28.0 $\pm$ 12.6 (3)			

fraction remains stable (Fig. 6a). Presumably the  $^3\text{H-CH}_4$  is lost through diffusion through the stoppers. This loss results in an increase of the ratio ( $^3\text{H-H}_2\text{O}/^3\text{H-CH}_4 + ^3\text{H-H}_2\text{O}$ ; Fig. 6b). This increase of the ratio will result in an overestimation of the MOX rate by 20–40%.

Thus, samples should be analyzed within 3–4 d, or if this is not possible an overestimation of the MOX rate of approx. 20% has to be accepted.

**Total radioactivity ( $^3\text{H-CH}_4$  and  $^3\text{H-H}_2\text{O}$ ) of the sample**

After incubation, the total radioactivity ( $^3\text{H-CH}_4$  and  $^3\text{H-H}_2\text{O}$ ) that was added to the water sample has to be determined. We determined the total radioactivity in all bottles,

samples, and controls. This allowed for a better precision, as we found a high variability ( $> 10\%$ ) between different bottles.

However, as methane has a low solubility, it rapidly equilibrates with the headspace in the scintillation vial and can leak from the scintillation vial.  $^3\text{H-CH}_4$  in the headspace cannot be counted in a liquid scintillation counter. To measure the total radioactivity ( $^3\text{H-CH}_4$  and  $^3\text{H-H}_2\text{O}$ ) most accurately, we tested vigorous vs. gently mixing of a sample with scintillation cocktail, how long the mixed sample can be left standing before analysis, and the use of polyethylene vs. glass vials.

Vigorous shaking vs. gentle mixing was tested by adding one milliliter sample to five milliliter scintillation cocktail in

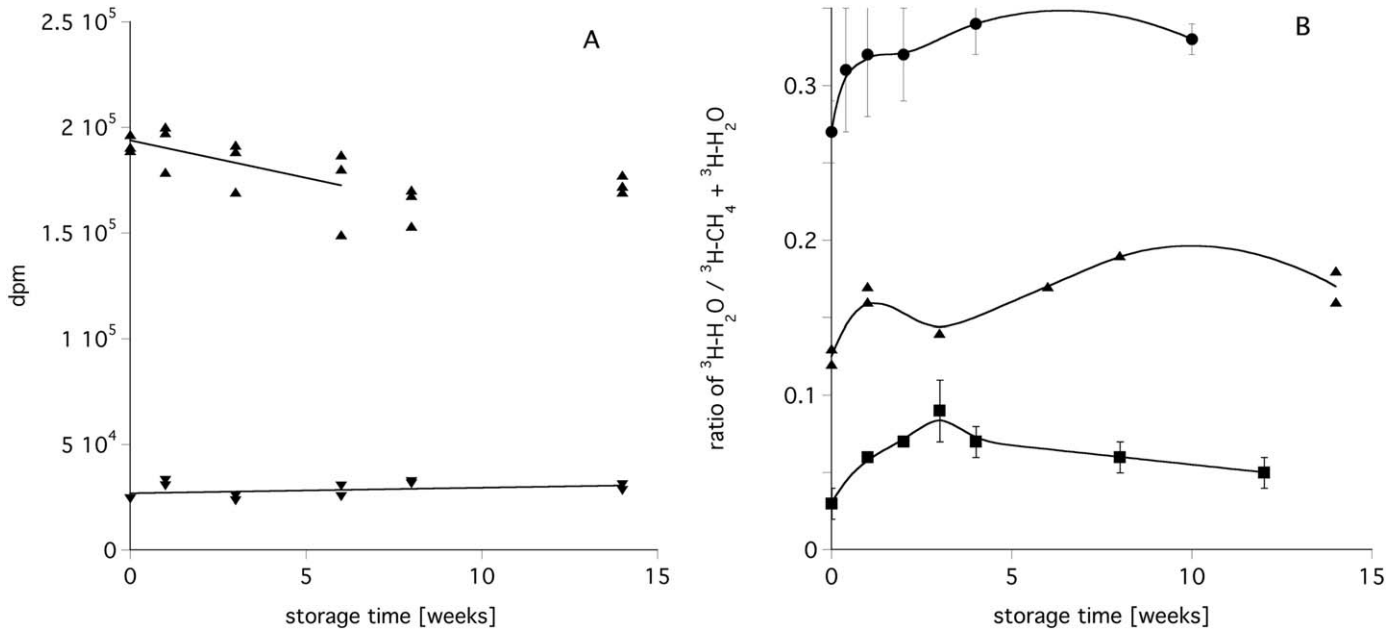


**Fig. 6.** The influence of the storage time on the radioactivity in the different fractions and on their ratio. Incubations of North Sea water were stopped after 24 h with 25% H<sub>2</sub>SO<sub>4</sub> and two to four bottles were analyzed immediately. The other samples were stored at 4°C and measured after the indicated time. (A) The radioactivity in dpm in the fraction ( $^3\text{H-CH}_4 + ^3\text{H-H}_2\text{O}$ ) with upward triangles and the radioactivity in the  $^3\text{H-H}_2\text{O}$  fraction with downward triangles. (B) The ratio ( $^3\text{H-H}_2\text{O}/^3\text{H-CH}_4 + ^3\text{H-H}_2\text{O}$ ) of three experiments, the triangles are from the same experiment shown in figure A.

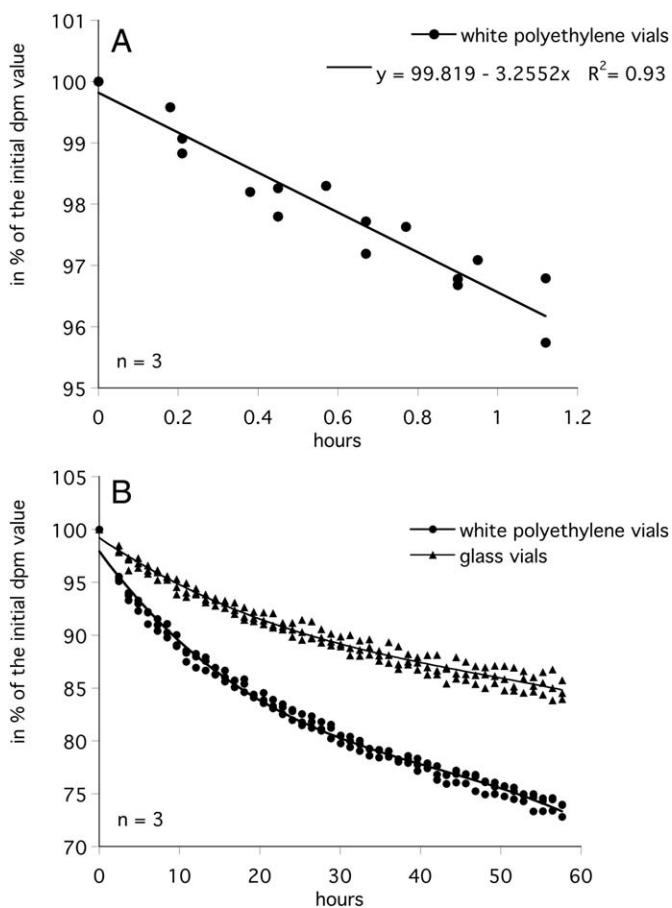


**Fig. 7.** Loss of  $^3\text{H-CH}_4$  from the total radioactivity ( $^3\text{H-CH}_4$  and  $^3\text{H-H}_2\text{O}$ ) in a scintillation vial with time. The scintillation vials contained a two milliliter subsample and five milliliter scintillation cocktail. The same vials were counted at different times.

each of two scintillation vials. One of the vials was gently turned upside down 3–4 times whereas the other was vigorously shaken by hand. The results show on average 7% less radioactivity in the vigorously shaken samples than in the gently mixed samples (Supporting Information 1). Vigorous shaking of the samples with the cocktail, thus, leads to a faster equilibration and higher leakage; therefore, mixing should be accomplished gently.

Furthermore, we observed that the total radioactivity rapidly decreases over time after addition of the scintillation cocktail and mixing (Fig. 7). Glass vials were found to have a slightly better performance than polyethylene vials. In glass vials, the total radioactivity decreased by  $\sim 15\%$  within 60 h, whereas in polyethylene vials radioactivity was reduced by 25% in 60 h. Already in the first hour, 4% of the total radioactivity is lost using polyethylene vials.

As the loss of radioactivity is due to equilibration between the fluid and the gas phase, the loss depends on the methane concentration in the vial, and might be lower at low methane concentrations. However, the experiments show,

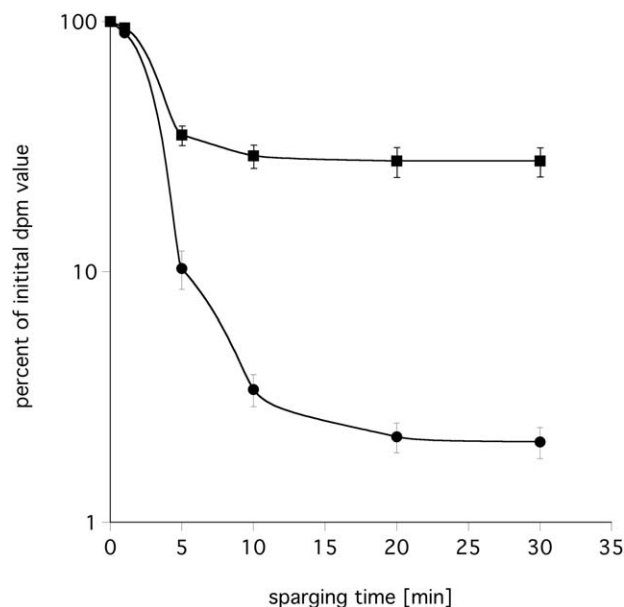


**Fig. 8.** Identification of the necessary sparging time to remove not microbially oxidized  $^3\text{H-CH}_4$ . Elbe water (squares,  $n = 3$ ) and North Sea water (circles,  $n = 3$ ) samples were incubated for 24 h and stopped by adding a poison. Radioactivity was measured after different times of sparging. Note the logarithmic scale of the y-axis.

that samples should be immediately counted after mixing. Further, we recommend to open and process less than 10 samples at once and set the counting time to 1–3 min as otherwise the total radioactivity of the last sample analyzed is biased due to  $^3\text{H-CH}_4$  leakage in the headspace.

### Radioactivity of the water fraction ( $^3\text{H-H}_2\text{O}$ )

To determine the amount of water that has been produced by the methanotrophic bacteria through the oxidation of methane, the radioactivity of the  $^3\text{H-H}_2\text{O}$  has to be quantified (Table 1). Therefore, the remaining  $^3\text{H-CH}_4$  has to be removed from the sample, which can be done by sparging the sample with nitrogen or air. We moistened the air by directing it through a washing flask to prevent evaporation of sample water. However, this effect appears negligible and accounts for  $< 0.2\%$  of the  $^3\text{H-H}_2\text{O}$  if one assumes an even distribution of the  $^3\text{H-CH}_4$  in the sample, an evaporation rate of  $200 \text{ g water m}^{-2} \text{ h}^{-1}$  and a sparging time of 30 min.

To test for the appropriate time to remove all of the  $^3\text{H-CH}_4$ , we sparged samples with a high and low activity for 5–30 min, that is, Elbe water and North Sea water, respectively. In the active samples about 28% of the added  $^3\text{H-CH}_4$  was found in the water fraction. In the less active samples, only 2% of the  $^3\text{H-CH}_4$  was found in the water fraction. In both cases, a stable counting was reached after 20–30 min of sparging (Fig. 8).

In contrast to the total radioactivity ( $^3\text{H-CH}_4$  and  $^3\text{H-H}_2\text{O}$ ), the radioactivity of the  $^3\text{H-H}_2\text{O}$  in the scintillation vial was stable over time (70 h, Supporting Information 2).



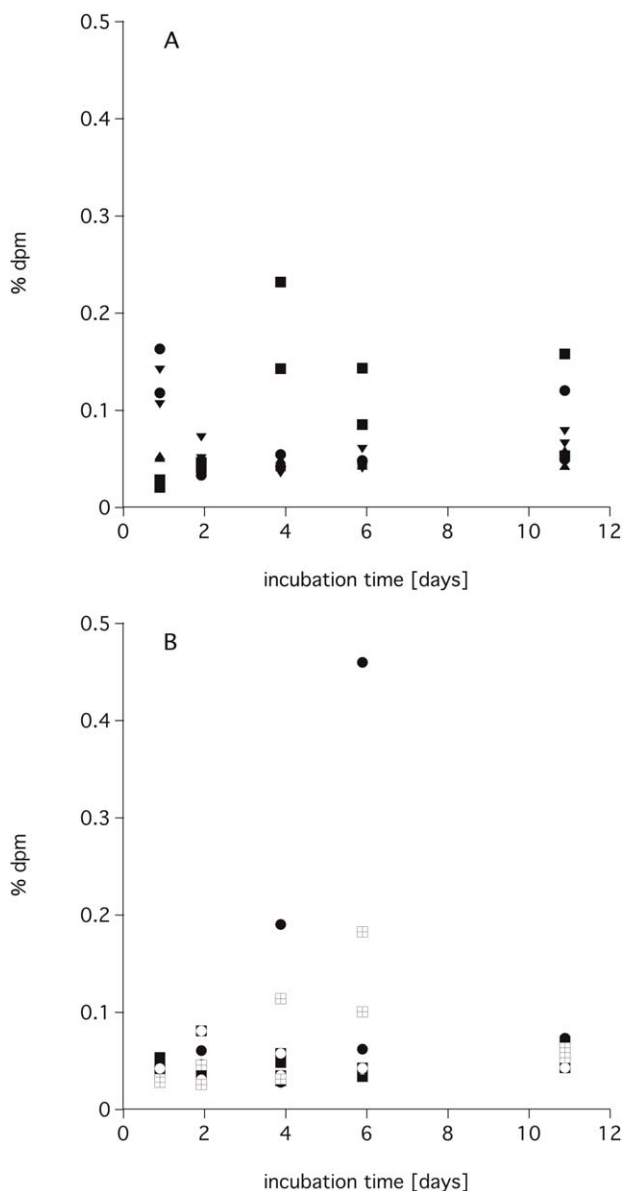


**Fig. 9.** Percent of  $^3\text{H}$ -tracer remaining in autoclaved water after incubation and sparging for 30 min to remove  $^3\text{H-CH}_4$ . Samples were stored at  $10^\circ\text{C}$  for up to 11 d. (A) Incubations with different salt concentrations: Milli Q (downward triangles), tap water (squares), seawater (circles), and brine (upward triangles). (B) Incubations with different pH: tap water with pH 5 (filled circles) and 9 (engulfed circles), seawater with pH 5 (filled squares) and 9 (crossed squares).

Therefore, the counting time can be extended to 10 min, to get a better statistical quality of the counts. The 2% sigma value as measured by the liquid scintillation counter for a given counting time decreased from 2% at 1 min to 0.6% at 10 min counting time.

### Storage of the $^3\text{H-CH}_4$ tracer

Because  $^3\text{H}$ -compounds generally have a high specific activity and, thus, a high radioactive decomposition rate,

this section provides advice on the optimal conditions for storing the  $^3\text{H-CH}_4$  tracer. Decomposition is the interaction of emitted particles with the immediate surroundings and/or with the molecules of the labeled compound causing destruction of the labeled substance. To lessen the decomposition, it is necessary to keep the number of interactions as low as possible. This can be achieved by storing the tracer at low temperatures and by dilution of the tracer. For the  $^3\text{H-CH}_4$  tracer dilution from the original ampoule, we recommend to use nitrogen, instead of air. In this way, reactions with  $\text{OH}$  and other compounds of the air will not occur. If the  $^3\text{H-CH}_4$  tracer is to be used over months, it is best to have subsamples in a number of vials. This way, vials to be used later can be kept in the refrigerator to avoid reopening and warming/cooling cycles. Furthermore,  $^3\text{H-CH}_4$  tracer is commonly stored on saturated salt solution, which decreases the likelihood of formation of reactive species. The water molecules surround the highly charged  $\text{Na}^+$  and  $\text{Cl}^-$  ions, increasing the structure of water and reducing the number of “free” water molecules, which can form reactive species such as  $\text{OH}^-$  radicals (Emerson and Hedges 2009).

### Background $^3\text{H-H}_2\text{O}$

Some of the  $^3\text{H-H}_2\text{O}$  is often suggested not to result from microbial MOX but from isotopic exchange reactions or decomposition of the tracer. Salinity and reactive species (e.g.,  $\text{OH}^-$ ,  $\text{H}^+$ ) are assumed to influence these processes (see storage of the tracer). That is, background  $^3\text{H-H}_2\text{O}$  is supposed to be higher in less saline water because more “free” water molecules are around, which are broken by radiation to, for example,  $\text{OH}^-$  and  $\text{H}^+$  ions, and react with the tracer forming  $^3\text{H-H}_2\text{O}$ . Similarly, pH modifies water to contain more reactive species. To test the influence of (i) salinity and (ii) pH on the concentration and stability of the background  $^3\text{H-H}_2\text{O}$ , we autoclaved water (deionized water, freshwater, seawater, a saturated salt solution, and freshwaters and seawaters with different pHs) to assure that all microbial activity is stopped. Then, we added the same amount of tracer to all samples. The samples were subsequently incubated in the dark at  $10^\circ\text{C}$  for up to 11 d. The results show no significant differences between the different setups, nor a significant change of the background value over time (Fig. 9). Apparently neither the availability of “free” water molecules in low salinity water, nor the increase in  $\text{H}^+$  (acidic water) or  $\text{OH}^-$  ions (basic water) led to elevated concentrations of  $^3\text{H-H}_2\text{O}$  over the 11-d time period. Therefore, the isotopic exchange reaction and decomposition of the  $^3\text{H-CH}_4$  tracer is negligible over typical time periods of incubations (hours to 3 d).

### Methane concentrations

The methane concentration is crucial for the calculation of the MOX rate. However, the concentrations can be determined either in separate bottles, in the control bottles or in the sample itself. The first possibility represents the in situ concentrations, while in the other ones, methane

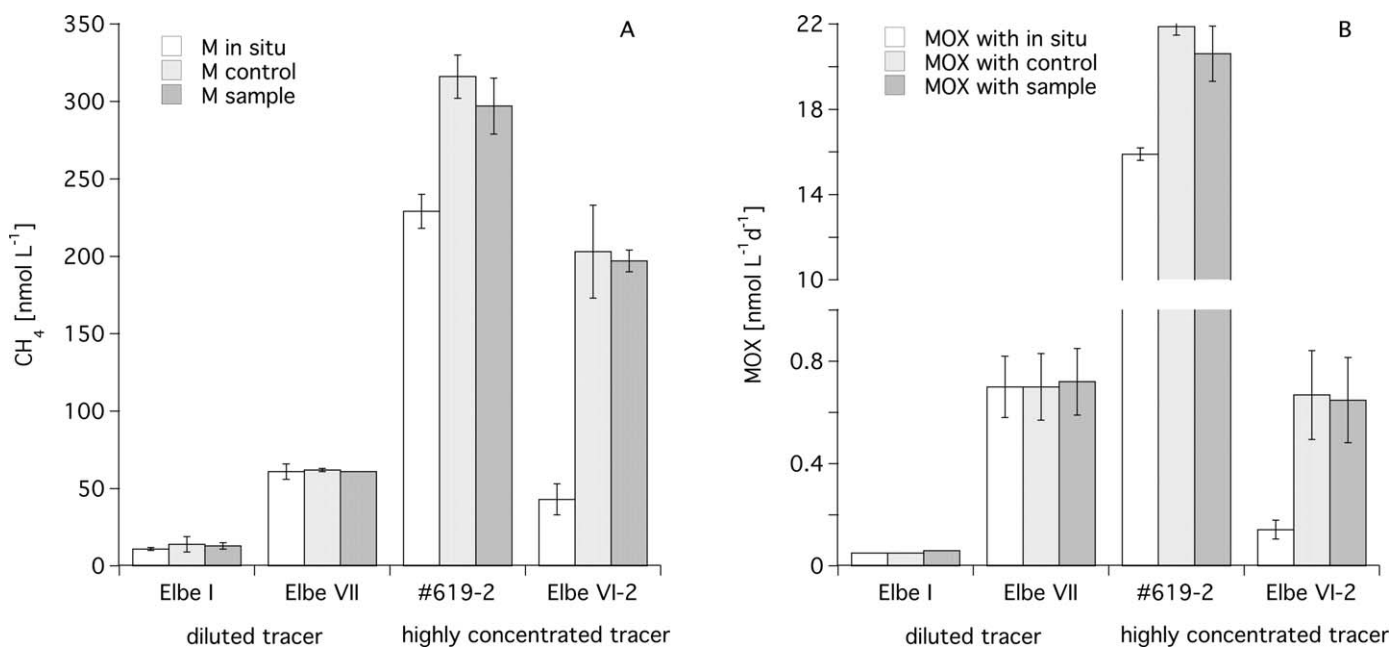


**Fig. 10.** Methane concentrations measured in a separate water samples, in control bottles, and samples bottles, the latter two contain tracer (A). MOX rates calculated with the corresponding in situ methane concentrations, the methane concentrations in the control and sample bottles (B). North Sea and Elbe water was collected for this experiment. Note the break in the y-axis.

concentrations are altered due to the addition of  $^3\text{H-CH}_4$ . The addition of  $^3\text{H-CH}_4$  should not increase the in situ methane concentrations significantly.

In several sets of samples, we determined the methane concentration (i) in separate bottles, (ii) in the killed controls, and (iii) in the sample bottles. Adding a diluted  $^3\text{H-CH}_4$  ( $1 \times 10^{11} \text{ Bq mol}^{-1}$ ) increased the methane concentration in the samples and controls by 3  $\text{nmol l}^{-1}$  or to 103% and 135% of the in situ concentration (Fig. 10). Subsequently, the MOX rate calculated with the different methane concentrations also were very similar. However, on a second cruise the  $^3\text{H-CH}_4$  was more concentrated ( $5 \times 10^{12} \text{ Bq mol}^{-1}$ ) and the methane concentrations in the samples and controls increased 1.5–5 times (to 138% and 469% of the in situ concentration). Thus, the MOX rates calculated with the methane concentrations of the control or the sample increased also by 1.5–5 times and were 1.5–5 times faster than the MOX rate calculated with the in situ methane concentration (Fig. 10). The experiment shows that (1) an additional sample for analysis of the in situ concentration is the easiest and most accurate way to calculate MOX rates and (2) the methane concentration of the  $^3\text{H-CH}_4$ -tracer should be adjusted for low methane concentration environments.

Using the same dataset, MOX rates were calculated based on the difference in methane concentration between the sample and control bottles. As methane consumption only takes place in the sample but not in the control bottle. In samples with high methanotrophic activity, calculation of the MOX rate with the  $^3\text{H-CH}_4$ -tracer measurement vs. cal-

ulation of the difference in concentration were comparable ( $158 \pm 4 \text{ nmol L}^{-1} \text{ d}^{-1}$  vs.  $144 \pm 31 \text{ nmol L}^{-1} \text{ d}^{-1}$ ), however, at low activities the difference in methane concentrations were within the measurement error of the GC ( $0.8 \pm 2.4 \text{ nmol L}^{-1} \text{ d}^{-1}$ ) and, thus, not comparable with the radiotracer measurements ( $0.05 \pm 0.01 \text{ nmol L}^{-1} \text{ d}^{-1}$ ). The latter comparison illustrates, why tracer experiments are essential in determining aerobic MOX in waters with low methane waters where slow MOX rates are expected. In these waters, the change in methane concentration over time cannot be measured by GC.

#### MOX rate calculation with time series or single end point measurement

The MOX rate of a specific water sample can be calculated from a time series or as most often is the case from a single end-point measurement. During a time series, consumption of  $^3\text{H-CH}_4$  is measured after an incubation time of for example 0.5 d, 1 d, 2 d, 3 d, the slope of a linear regression of the fraction of the  $^3\text{H-CH}_4$  oxidized vs. time is used to calculate  $k'$  and then the MOX rate. The rate constant,  $k'$ , is, thus, determined from a dataset ( $n \geq 8$ ). In contrast, single end-point measurements derive  $k'$  from replicate samples ( $n \geq 2$ ). Commonly single end-point measurements are made assuming first-order kinetics, that is, the reaction depends solely on the availability of one substrate, which is methane in this case. Further, it is assumed that the cell population is not growing. To test the reliability of these assumptions, we compared  $k'$  derived from (i) a linear

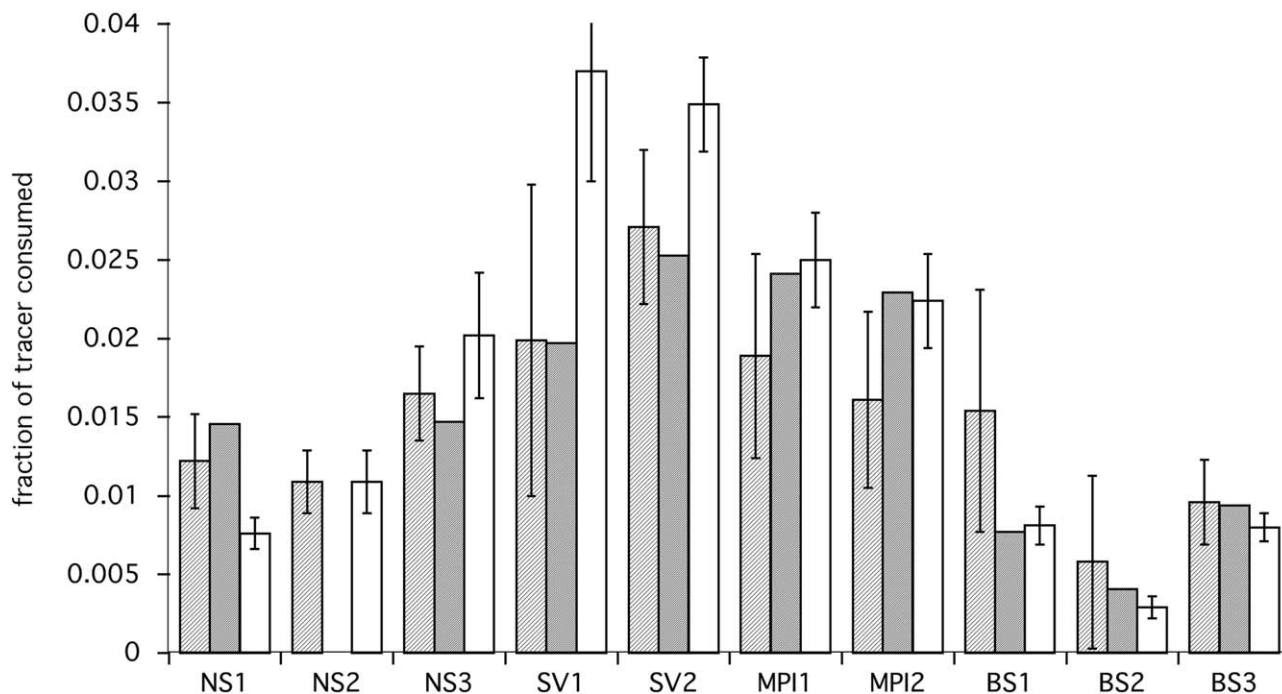


**Fig. 11.** Comparison of the fraction of consumed tracer as calculated either from a linear regression of a time series (white columns), from the average of 3–4 single time points (light shade columns) and from one single end point at 24 h (dark shaded column). Details of the calculation are described in the text. The calculations were applied for three samples from the North Sea (NS1, 2, 3), two samples from off Svalbard (SV1, 2) and for methane rich freshwater settings (MPI1, 2) and Bodensee (BS1, 2, 3).

regression of time series data, (ii) from the average of the time points of a time series, and (iii) the commonly used 24 h incubation. We used data from marine environments (North Sea and Svalbard), as well as freshwater environments (MPI-pond and Lake Constance), in total 10 datasets. Incubation times ranged from 2 h to 24 h for the freshwater samples and from one day to five days for the marine samples.

As a first step for the time series data, we tested if a linear regression sufficiently describes the data. For all datasets, the average of the residuals was equal to zero ( $t$ -test for “0”). Also the residuals were normally distributed (Shapiro–Wilk Normality Test with  $p = 0.01$ , except one dataset). This indicates that the difference from the measured data to the calculated line fit was randomly distributed and showed no systematic deviation. Comparing  $k'$  as calculated by (i) a linear regression or by (ii) average of single end points, revealed no significant difference (Wilcoxon Rank Sign Test for paired data,  $n = 10$ ,  $p = 0.34$ ), as also shown in Fig. 11.

In general only one single time point (i.e., 24 h) is used for MOX rate calculations. Thus, this one single time point calculation is included among the single time point calculations (see also Fig. 4). As shown in Fig. 11 these values range within the values for the linear regression and the single end point calculation and their standard deviations. On average the one single end point calculation was 5% different from

the linear regression calculation. Therefore, we assume that the above conclusions are also valid for single time point calculation, as long as this time point lies within the linear range (Fig. 4).

#### Detection limit

Control samples are frequently taken and are poisoned immediately after the addition of the  $^3\text{H-CH}_4$  and the “initial ratio” ( $^3\text{H-H}_2\text{O}/^3\text{H-CH}_4 + ^3\text{H-H}_2\text{O}$ ) is determined. The mean ( $x$ ) and the standard deviation ( $s$ ) of all controls sampled during different cruises in different areas were calculated and the limit of detection (LOD) was set as:

$$\text{LOD} = x + 3 \times s$$

All samples with the “initial ratio” below this LOD-value were considered as below the detection limit and had to be set as zero. We applied this strict rule to different datasets of MOX rates (Table 3) with methane concentrations ranging from background concentrations of  $1 \text{ nmol l}^{-1}$  to high seep concentrations of  $1456 \text{ nmol l}^{-1}$ . In some cases, 70% of the data were below the detection limit and had to be set to zero. The lowest detected value was  $0.001 \text{ nmol l}^{-1} \text{ d}^{-1}$  based on the datasets of Table 3.

The use of laboratory based vs. portable LSD may also influence the LOD. Especially at low activities the counting efficiency of the liquid scintillation counter may be critical.

**Table 3.** LOD calculated for datasets of different areas. The \* indicates samples which were measured with a portable Liquid scintillation counter.

Cruise, Year	Area	CH <sub>4</sub> (nmol L <sup>-1</sup> )	LOD MOX (nmol L <sup>-1</sup> d <sup>-1</sup> )	Data below LOD (%)
HE333, 2010	Svalbard	5–86	0.02	4
PO419, 2011	Svalbard	1–546	0.02*	68
HE406, 2013	North Sea	4–1456	0.02*	70
PS-ANTXXIX, 2013	South Georgia	1–56	0.001	38
HE413, 2014	North Sea	9–686	0.1*	11

For example, the same samples which were counted with a laboratory-based machine with 760 dpm and 815 dpm, retrieved only 189 dpm and 181 dpm with a portable liquid scintillation counter. While samples with higher counts (47,000 dpm) did not indicate any differences between the two liquid scintillation counters.

**Discussion**

Although it is known that methane is microbially oxidized in lakes and oceans and that this process reduces the gas flux into the atmosphere, only a small number of MOX data are available. <sup>3</sup>H-CH<sub>4</sub> being relatively new commercially available provides a convenient tracer to determine the MOX rate in natural waters. Compared to the <sup>14</sup>C-CH<sub>4</sub> method, the <sup>3</sup>H-CH<sub>4</sub> method requires minimal sample processing and few specialized equipment. However, as known from the common saying “the devil is in the details,” we

checked the method to produce a best practice guide hoping to encourage people to take up the method and indicating the important parameters that can cause large errors. Below, we first discuss the errors found during the method assessment before evaluating existing data.

**Error discussion**

We compared the different parameters causing uncertainties of the results as outlined in the assessment part by calculating for each tested modification the deviation from the common method in percent. For example, the deviation of the result caused by applying a 10 μL tracer bubble instead of the commonly used 100 μL tracer injection or the deviation caused by storing killed samples for 60 h in contrast to processing samples right after incubation as commonly done (Fig. 12). We also applied different methane concentrations to calculate the MOX rate, but recommend using the real in situ methane concentration as measured in separate bottles.

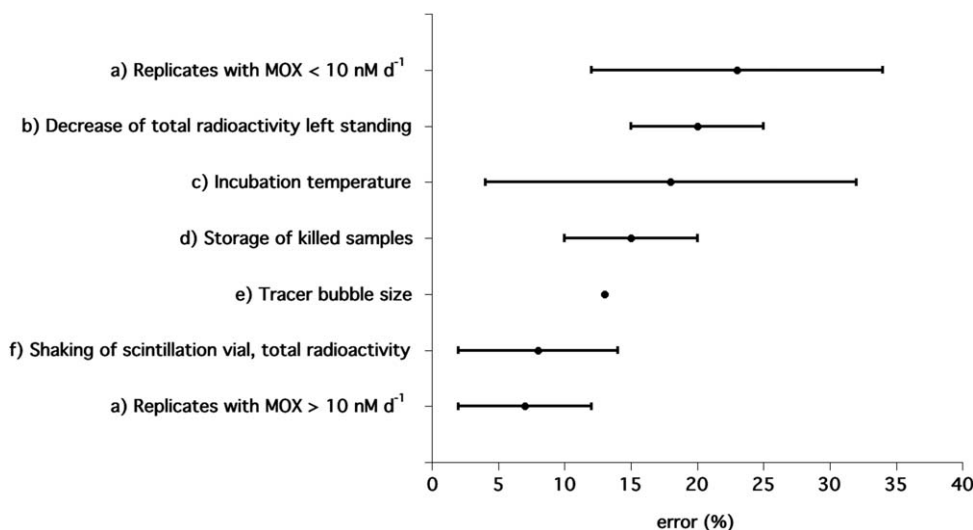


**Fig. 12.** Mean and standard deviation of error associated with different parts of the method: (A) error of replicates indicates the difference from the mean value, (B) decrease of total activity left standing shows the difference between measuring the total activity right after stopping the incubation and measuring after 60 h left standing, (C) incubation temperature illustrates the error of MOX rates if incubation temperatures differ by 1–5°C and Q<sub>10</sub> ranges between 1.52 and 1.75, (D) storage of killed samples illustrates the error associated with storing a sample instead of rapid post-processing, (E) bubble size indicates the measured difference between a 100 μL bubble and a 10 μL bubble, (F) shaking of scintillation vials indicates the error associated with vigorous shaking of the total activity sample in a scintillation vial.



Otherwise the MOX rates will increase by the same factor as the methane concentrations are increased. However, we did not include this comparison in Fig. 12 as we think this is rather a calculation error than a methodological error.

The largest uncertainty is due to the precision of the MOX rate measurements in waters with low methanotrophic activity (i.e., MOX-rates  $< 10 \text{ mol l}^{-1} \text{ d}^{-1}$ ). By increasing the number of replicates, the precision of the data can be improved, however, at high costs of work effort and material.

This large uncertainty can be viewed as the total error of MOX rates that consists of the error of each step of the method and the heterogeneity of the methanotrophic population in a water sample. This total error is influenced by the following uncertainties which apparently impact low rate measurements more than high rate measurements. The largest impact on the total error is caused by measuring of the total radioactivity ( $^3\text{H-CH}_4$  and  $^3\text{H-H}_2\text{O}$ ) not right after opening a sample. The second largest influence is due to incorrect incubation temperature. By incubating samples at temperatures as close as possible to the in situ temperature over- or underestimation of MOX rate can be avoided. The error associated with temperature can also be corrected using published  $Q_{10}$  factors. However, as the data base for methanotrophic  $Q_{10}$  is very small, we recommend to incubate the samples as close as possible to the in situ temperature or to determine a  $Q_{10}$  for the respective environment. A similarly high error results from the storage of killed samples in comparison to postprocessing the samples right after incubation. The fourth largest error results from the size of the injected  $^3\text{H-CH}_4$  bubble and minor errors are due to vigorous shaking of the scintillation vial and subsequent counting of the total activity.

Some of these errors are easily avoidable while others can only be limited with more effort. Errors that can be avoided are: (1) measuring the total radioactivity ( $^3\text{H-CH}_4$  and  $^3\text{H-H}_2\text{O}$ ) right after opening the sample, (2) not leaving killed samples standing for later analysis, (3) using an appropriate  $^3\text{H-CH}_4$  bubble volume, and (4) shaking the total radioactivity ( $^3\text{H-CH}_4$  and  $^3\text{H-H}_2\text{O}$ ) scintillation mixture gently. The other errors: (1) precision of low activity samples, (2) incubation at in situ temperature or derivation of  $Q_{10}$ , and (3) derivation of a more accurate  $k'$  by implementing a time series, can also be minimized, but only by processing more samples. It depends on the scientific question and the according precision of the analysis needed, if the additional work and also the additional radioactive waste justify the higher effort.

In contrast to the parameters discussed above, bottle size, background, and produced  $^3\text{H-H}_2\text{O}$ , as well as shaking of the samples during incubation cause insignificant MOX rate errors in natural waters. Bottle size insignificantly altered MOX rate measurements; thus, bottle size can be reduced to lessen radioactive waste. Measurements of background  $^3\text{H-H}_2\text{O}$  in microbial inactive waters remained low over 11 d.

Therefore, the chemical reaction, that is, self-decomposition and ionic exchange are negligible in the time frame of a typical incubation ( $< 3 \text{ d}$ ). If killed controls show a high  $^3\text{H-H}_2\text{O}$  content, microbial metabolism was apparently not efficiently stopped as was shown by Boden and Murrell (2011), who investigated methanotrophic resistivity to  $\text{HgCl}_2$ . Not only the background, but also the produced  $^3\text{H-H}_2\text{O}$  during microbial MOX was found stable over time, thus, these measurements can be delayed, for example, for on-shore analysis. Finally, shaking of the samples during incubation was not found to be relevant and is, thus, not necessary.

Other details of the method investigated resulted in suggestions for best practice to determine MOX rates. Stoppers should consist of halogenated butyl rubber. The tracer is best stored on saturated NaCl-solution, diluted in  $\text{N}_2$  and at low temperatures (refrigerator). The incubation time is best determined by conducting a time series and the sparging time should be 30 min. We also recommend to determine the in situ methane concentration used for MOX rate calculations in separate bottles. Thus, one does not need to correct for increased methane concentrations through the addition of  $^3\text{H-CH}_4$  nor for decreased methane concentrations due to methane consumption by methanotrophs.

#### Existing data evaluation

MOX rates have been measured using  $^{14}\text{C-CH}_4$  and  $^3\text{H-CH}_4$ ; data which cannot be readily compared. In the 20<sup>th</sup> century, water column MOX rates were determined using  $^{14}\text{C-CH}_4$  (Scranton and Brewer 1978; Ward et al. 1987) while the  $^3\text{H-CH}_4$  moved toward becoming commercial accessible in the 21<sup>st</sup> century. The data are not comparable as 100-fold more methane is added to a sample using  $^{14}\text{C-CH}_4$  compared to  $^3\text{H-CH}_4$  resulting in potential rates at elevated substrate concentration and near in situ rates, respectively. This difference was evaluated in water samples from Storfjorden and discussed in Mau et al. (2013).

For both tracers, the precision of the rate measurement in waters of low methane concentrations and activity appears to be the main uncertainty. In this study, we found the precision of MOX rates in waters of low methanotrophic activity to be the largest error, which might be due to the general higher error associated with low concentration experiments but could also be due to tracer-back-flux as reported for the anaerobic oxidation of methane (Holler et al. 2011). Also Bleses et al. (2014) and Jakobs et al. (2013) indicate a great variability in low concentration-samples using  $^{14}\text{C-CH}_4$ . However, existing publications all include measurements of replicate samples stating the precision. In most studies, duplicate or triplicate sampling is performed. When duplicate samples are used, both data points are shown (Gentz et al. 2013; Mau et al. 2013). Studies with triplicate sampling either show the error bars (Bleses et al. 2014) or provide the standard deviation (Jakobs et al. 2013). Hence, the data is of good quality especially when considering rate measurements

in the sediment where duplicate or triplicate measurements are not feasible.

In contrast to the precision of the measurements, the difference between in situ temperature and incubation temperature was hardly ever corrected, even though we found temperature to cause the second largest influence on error of MOX rates. Most often samples are incubated at a temperature that is close to the in situ temperature, but usually not exactly at in situ temperature. It is normally also not feasible to incubate all samples at in situ temperature, especially in summer when surface ocean temperatures are significantly elevated in comparison to deep water temperatures. Even if two or three incubators are available and set to different temperatures, some water samples are still not incubated at in situ temperatures. Besides, all cooling devices have cooling cycles which might cause temperature variations of up to 5°C (refrigerator). It would be also helpful to monitor more exactly the incubation temperature. Using the  $Q_{10}$  correction underestimation or overestimation of the MOX rates can be evaluated, although published  $Q_{10}$  values are bulk values and might differ between regions due to the presence of different methanotrophic communities. Certainly, more  $Q_{10}$  need to be derived to overcome this insufficient correction of MOX rates.

Another drawback of existing datasets is that no detection limit (LOD) was provided so far. Therefore, very low rates were published, which are most likely below the detection limit. We calculated LOD to be on the order of 0.001 nmol  $\text{L}^{-1} \text{d}^{-1}$  to 0.01 nmol  $\text{L}^{-1} \text{d}^{-1}$  and recommend to use Eq. 5 to derive the detection limit and use only the data that show significant MOX.

### Comments and recommendations

Based on the experiments performed for this study, we recommend considering the following aspects when planning MOX rate measurements in an unknown environment. With a time series, the assumption of first-order kinetics can be checked and the appropriate incubation time can be defined. We encountered a rather high variability of the MOX rates, thus, at least three parallel samples are necessary to obtain a sufficient precision. Especially in methane poor environments with low activities the aspect of the detection limit has often been neglected. Therefore, a sufficient number of killed controls have to be setup allowing to distinguish between “real” methane consumption and background noise.

In our study, we investigated some of the important aspects of MOX measurements. However, even when writing the manuscript, we are well aware and realized that more aspects still would be interesting or important to look at. Such aspects could be: Is there a difference when poisoning the controls before or after the tracer addition? What is the influence of different scintillation cocktails and different liquid scintillation counter on the rates? Are there differences

between MOX measurements when using gaseous  $^3\text{H-CH}_4$  compared to an aqueous tracer solution? The kinetics of MOX in natural waters is still not well-known, as most studies were done with pure cultures of methanotrophs or with soil samples. The priming effect (injection of additional methane and, thus, increasing substrate concentrations) could be tested with nonlabeled methane as well as with labeled methane as was done only by Mau et al. (2013) so far. As with all/many methods an interlaboratory comparison of MOX measurements would be very instructive.

Nevertheless, with our study we hope to improve and to encourage future measurements of MOX rates in different environments. We also hope to develop a standard procedure of MOX rate measurements to make data of MOX better comparable.

### References

- Abril, G., M.-V. Commarieu, and F. Guérin. 2007. Enhanced methane oxidation in an estuarine turbidity maximum. *Limnol. Oceanogr.* **52**: 470–475. doi:10.2307/40006095
- Abril, G., and N. Iversen. 2002. Methane dynamics in a shallow non-tidal estuary (Randers Fjord, Denmark). *Mar. Ecol. Prog. Ser.* **230**: 171–181. doi:10.3354/meps230171
- Angelis, M. A. D., M. D. Liley, E. J. Olson, and J. A. Baross. 1993. Methane oxidation in deep-sea hydrothermal plumes of the Endeavour Segment of the Juan da Fuca Ridge. *Deep-Sea Res.* **40**: 1169–1186. doi:10.1016/0967-0637(93)90132-M
- Bange, H. W., U. H. Bartell, S. Rapsomanikis, and M. O. Andreae. 1994. Methane in the Baltic and North Seas and a reassessment of the marine emissions of methane. *Glob. Biogeochem. Cycl.* **8**: 465–480.
- Bastviken, D., J. Ejlertsson, I. Sundh, and L. Tranvik. 2002. Measurement of methane oxidation in lakes: A comparison of methods. *Environ. Sci. Technol.* **36**: 3354–3361. doi:10.1021/es010311p
- Bastviken, D., L. J. Tranvik, J. A. Downing, P. M. Crill, and A. Enrich-Prast. 2011. Freshwater methane emissions offset the continental carbon sink. *Science* **331**: 50–50. doi:10.1126/science.1196808
- Blees, J., and others. 2014. Micro-aerobic bacterial methane oxidation in the chemocline and anoxic water column of deep south-Alpine Lake Lugano (Switzerland). *Limnol. Oceanogr.* **59**: 311–324. doi:10.4319/lo.2014.59.2.0311
- Boden, R., and others. 2011. Complete genome sequence of the aerobic marine methanotroph methylomonas methanica MC09. *J. Bacteriol.* **193**: 7001–7002. doi:10.1128/JB.06267-11
- Bowman, J. 2006. The methanotrophs—the families methylcocccaceae and methylocystaceae, p. 266–289. *In* Prokaryotes. Springer.
- Button, D. K. 1991. Biochemical basis for whole-cell uptake kinetics: Specific affinity, oligotrophic capacity, and the

- meaning of the Michaelis constant. *Appl. Environ. Microbiol.* **57**: 2033–2038.
- Damm, E., E. Helmke, S. Thoms, U. Schauer, E. Nöthig, K. Bakker, and R. P. Kiene. 2010. Methane production in aerobic oligotrophic surface water in the central Arctic Ocean. *Biogeosciences* **7**: 1099–1108. doi:10.5194/bg-7-1099-2010
- Ding, H., D. L. Valentine. 2008. Methanotrophic bacteria occupy benthic microbial mats in shallow marine hydrocarbon seeps, Coal Oil Point, California. *J. Geophys. Res.* **113**: G01015, 2008. doi:0.1029/2007JG000537
- Ducklow, H. W., O. Schofield, M. Vernet, S. Stammerjohn, and M. Erickson. 2012. Multiscale control of bacterial production by phytoplankton dynamics and sea ice along the western Antarctic Peninsula: A regional and decadal investigation. *J. Mar. Syst.* **98**: 26–39. doi:10.1016/j.jmarsys.2012.03.003
- Dumestre, J. F., J. Guézennec, C. G. Lacaux, R. Delmas, S. Richard, and L. Labroue. 1999. Influence of light intensity on methanotrophic bacterial activity in Petit Saut Reservoir, French Guiana. *Appl. Environ. Microbiol.* **65**: 534–539.
- Dunfield, P., R. Knowles, R. Dumont, and T. R. Moore. 1993. Methane production and consumption in temperate and subarctic peat soils: Response to temperature and pH. *Soil Biol. Biochem.* **25**: 321–326. doi:10.1016/0038-0717(93)90130-4
- Emerson, S., and J. Hedges. 2009. *Chemical oceanography and the marine carbon cycle*. Cambridge Univ. Press.
- Gentz, T., E. Damm, J. S. Von Deimling, S. Mau, D. F. McGinnis, and M. Schlüter. 2013. A water column study of methane around gas flares located at the West Spitsbergen continental margin. *Cont. Shelf Res.* **72**: 107–118. doi:10.1016/j.csr.2013.07.013
- Heeschen, K. U., R. S. Keir, G. Rehder, O. Klatt, and E. Suess. 2004. Methane dynamics in the Weddell Sea determined via stable isotope ratios and CFC-11. *Glob. Biogeochem. Cycl.* **18**: GB2012 2011–2018. doi:10.1029/2003GB002151
- Heintz, M. B., S. Mau, and D. L. Valentine. 2012. Physical control on methanotrophic potential in waters of the Santa Monica Basin, Southern California. *Limnol. Oceanogr.* **57**: 420–432. doi:10.4319/lo.2012.57.2.0420
- Holler, T., and others. 2011. Carbon and sulfur back flux during anaerobic microbial oxidation of methane and coupled sulfate reduction. *Proc. Natl. Acad. Sci. USA* **108**: E1484–E1490. doi:10.1073/pnas.1106032108
- Horak, R. E. A., and others. 2013. Ammonia oxidation kinetics and temperature sensitivity of a natural marine community dominated by Archaea. *ISME J.* **7**: 2023–2033. doi:10.1038/ismej.2013.75
- IPCC, 2013. Carbon and other biogeochemical cycles. In T. F. Stocker, D. Qin, G.-K. Plattner, M. Tignor, S. K. Allen, J. Boschung, A. Nauels, Y. Xia, V. Bex, and P. M. Midgley [eds.], *Climate Change 2013: The Physical Science Basis*. Contribution of Working Group I to the Fifth Assessment Report of the Intergovernmental Panel on Climate Change Cambridge Univ. Press.
- Jakobs, G., G. Rehder, G. Jost, K. Kießlich, M. Labrenz, and O. Schmale. 2013. Comparative studies of pelagic microbial methane oxidation within the redox zones of the Gotland Deep and Landsort Deep (central Baltic Sea). *Biogeosciences* **10**: 7863–7875. doi:10.5194/bg-10-7863-2013
- Jones, R. D. 1991. Carbon monoxide and methane distribution and consumption in the photic zone of the Sargasso Sea. *Deep-Sea Res.* **38**: 625–635. doi:10.1016/0198-0149(91)90002-W
- Jørgensen, B. B. 1978. A comparison of methods for the quantification of bacterial sulfate reduction in coastal marine sediments. I. Measurements with radiotracer techniques. *Geomicrobiol. J.* **1**: 11–64.
- Karl, D. M., L. Beversdorf, K. M. Bjoerkman, M. J. Church, A. Martinez, and E. F. Delong. 2008. Aerobic production of methane in the sea. *Nat. Geosci.* **1**: 473–478. doi:10.1038/ngeo234
- Koschel, R. 1980. Untersuchungen zur Phosphataffinität des Planktons in der euphotischen Zone von Seen. *Limnologica* **12**: 141–145.
- Krüger, M., T. Treude, H. Wolters, K. Nauhaus, and A. Boetius. 2005. Microbial methane turnover in different marine habitats. *Palaeogeogr. Palaeoclimatol. Palaeoecol.* **227**: 6–17. doi:10.1016/j.palaeo.2005.04.031
- Mau, S., J. Blees, E. Helmke, H. Niemann, and E. Damm. 2013. Vertical distribution of methane oxidation and methanotrophic response to elevated methane concentrations in stratified waters of the Arctic fjord Storfjorden (Svalbard, Norway). *Biogeosciences* **10**: 6267–6278. doi:10.5194/bg-10-6267-2013
- Metcalf, W. W., and others. 2012. Synthesis of methylphosphonic acid by marine microbes: A source for methane in the aerobic ocean. *Science* **337**: 1104–1107. doi:10.1126/science.1219875
- Niemann, H., and others. 2015. Toxic effects of lab-grade butyl rubber stoppers on aerobic methane oxidation. *Limnol. Oceanogr.: Methods* **13**: 40–52. doi:10.1002/lom3.10005
- Pack, M. A., M. B. Heintz, W. S. Reeburgh, S. E. Trumbore, D. L. Valentine, X. Xu, and E. R. M. Druffel. 2011. A method for measuring methane oxidation rates using low levels of  $^{14}\text{C}$ -labeled methane and accelerator mass spectrometry. *Limnol. Oceanogr.: Methods* **9**: 245–260. doi:10.4319/lom.2011.9.245
- Rahalkar, M., and J. Deutzmann, B. Schink, and I. Bussmann. 2009. Abundance and activity of methanotrophic bacteria in littoral and profundal sediments of Lake Constance. *Appl. Environ. Microbiol.* **75**: 119–126. doi:10.1128/AEM.01350-08

- Raven, J. A., and R. J. Geider. 1988. Temperature and algal growth. *New Phytol.* **110**: 441–461. doi:[10.1111/j.1469-8137.1988.tb00282.x](https://doi.org/10.1111/j.1469-8137.1988.tb00282.x)
- Reeburgh, W. 2007. Oceanic methane biogeochemistry. *Chem. Rev.* **107**: 486–513. doi:[10.1021/cr050362v](https://doi.org/10.1021/cr050362v)
- Reeburgh, W. S., B. B. Ward, S. C. Whalen, K. A. Sandbeck, K. A. Kilpatrick, and L. J. Kerkhof. 1992. Black Sea methane geochemistry. *Deep-Sea Res.* **38**: 1189–1210. doi:[10.1128/AEM.71.12.8099-8106.2005](https://doi.org/10.1128/AEM.71.12.8099-8106.2005)
- Rehder, G., R. Keir, E. Suess, and M. Rhein. 1999. Methane in the northern Atlantic controlled by microbial oxidation and atmospheric history. *Geophys. Res. Lett.* **26**: 587–590. doi:[10.1029/1999GL900049](https://doi.org/10.1029/1999GL900049)
- Schubert, C. J., and others. 2010. Oxidation and emission of methane in a monomictic lake (Rotsee, Switzerland). *Aquat. Sci.* **72**: 455–466. doi:[10.1007/s00027-010-0148-5](https://doi.org/10.1007/s00027-010-0148-5)
- Scranton, M. I., and P. G. Brewer. 1978. Consumption of dissolved methane in the deep ocean. *Limnol. Oceanogr.* **23**: 1207–1213. doi:[10.4319/lo.1978.23.6.1207](https://doi.org/10.4319/lo.1978.23.6.1207)
- Simon, M., S. Billerbeck, D. Kessler, N. Selje, and A. Schlingloff. 2012. Bacterioplankton communities in the Southern Ocean: Composition and growth response to various substrate regimes. *Aquat. Microb. Ecol.* **68**: 13–28. doi:[10.3354/ame01597](https://doi.org/10.3354/ame01597)
- Tang, K. W., D. F. McGinnis, K. Frindte, V. Brüchert, and H. P. Grossart. 2014. Paradox reconsidered: Methane oversaturation in well-oxygenated lake waters. *Limnol. Oceanogr.* **59**: 275–284. doi:[10.4319/lo.2014.59.1.0275](https://doi.org/10.4319/lo.2014.59.1.0275)
- Tissot, B. P., and D. H. Welte. 1984. *Petroleum formation and occurrence*. Springer Verlag, Heidelberg.
- Tsutsumi, M., H. Kojima, and M. Fukui. 2012. Vertical profiles of abundance and potential activity of methane-oxidizing bacteria in sediment of Lake Biwa, Japan. *Microbes Environ.*
- Valentine, D. L., D. C. Blanton, W. S. Reeburgh, and M. Kastner. 2001. Water column methane oxidation adjacent to an area of active hydrate dissociation, Eel river Basin. *Geochim. Cosmochim. Acta* **65**: 2633–2640. doi:[10.1016/S0016-7037\(01\)00625-1](https://doi.org/10.1016/S0016-7037(01)00625-1)
- Ward, B. B., K. A. Kilpatrick, P. C. Novelli, and M. I. Scranton. 1987. Methane oxidation and methane fluxes in the ocean surface layer and deep anoxic waters. *Nature* **327**: 226–229. doi:[10.1038/327226a0](https://doi.org/10.1038/327226a0)

### Acknowledgments

Many thanks are given to the scientific parties and crews of the research vessels Heincke, Polarstern, Poseidon, Prandtl, and Uthörn. We thank K.W. Klings for excellent technical assistance. We like to thank J. Brees, the laboratory of A. Boetius and D.L. Valentine for their help analyzing samples and providing equipment. We acknowledge the support of the PERGAMON for the initial workshop “Establishing standard protocols for the quantification of microbial methane oxidation rates in sediments and in the water column,” Kiel, June 2012. This work was partly funded through the project “Limitations of marine methane oxidation” funded by the DFG (Grant no. MA 3961/2-1). The work of A.M. was funded by the DAAD, by the Grant Agency of the Czech Republic (Grant no. 13-00243S) and a grant of the Faculty of Science, University of South Bohemia (GAJU 04-145/2013/P).

Submitted 22 September 2014

Revised 16 February 2015

Accepted 5 March 2015

Associate Editor: Dr. Paul Kemp